Quantifying spatial and temporal Holocene carbon accumulation in ombrotrophic peatlands of the Eastmain region, Quebec, Canada

Simon van Bellen

DÉCLIQUE UQAM-Hydro-Quebec Chair and Institut des Sciences de l'Environnement/GEOTOP, Université du Québec à Montréal, Succursale Centre-Ville, C.P. 8888, Montréal, Québec, H3C 3P8, Canada. Phone : +1 514 987 3000 #6680. E-mail : van_bellen.simon@courrier.uqam.ca

Pierre-Luc Dallaire

DÉCLIQUE UQAM-Hydro-Quebec Chair and Département de Géographie/GEOTOP, Université du Québec à Montréal, Succursale Centre-Ville, C.P. 8888, Montréal, Québec, H3C 3P8, Canada. Phone : +1 514 987 3000 #2771. E-mail : plucdal@hotmail.com

Michelle Garneau

DÉCLIQUE UQAM-Hydro-Quebec Chair and Département de Géographie/GEOTOP, Université du Québec à Montréal, Succursale Centre-Ville, C.P. 8888, Montréal, Québec, H3C 3P8, Canada. Phone : +1 514 987 3000 #1933. E-mail : garneau.michelle@uqam.ca

Yves Bergeron

NSERC-UQAT-UQAM industrial Chair in sustainable forest management, Université du Québec en Abitibi-Témiscamingue, 445 boulevard de l'Université, Rouyn-Noranda, Québec, J9X 5E4, Canada. Phone : +1 819 762 0971 #2347. E-mail : yves.bergeron@uqat.ca

Running title: Quantifying peatland C sequestration

Abstract

Northern peatlands represent important stocks of organic carbon (C). Peatland C dynamics have the potential to influence atmospheric greenhouse gas concentrations and are therefore of interest concerning future climate change. Quantification of Holocene variations in peat C accumulation rates is often based on a single, deep core. However, deep cores may overestimate accumulation rates when extrapolated to the ecosystem scale. We propose a reconstruction of C sequestration patterns based on multiple cores from three ombrotrophic peatlands in boreal Quebec, Canada. Both total C accumulation and temporal variations herein were quantified. Radiocarbon-dated stratigraphies from different sections resulted in peatland-specific age-depth models. Peatland initiation started rapidly after deglaciation around 7500 cal BP. Vertical accumulation slowed down in the course of the Holocene, whereas lateral expansion was rapid in the early stages but slowed down near mid-Holocene. Total C accumulation showed maximum rates between 5250 and 3500 cal BP with a regional mean Holocene apparent rate of 16.2 g m^{-2} yr^{-1}. The Eastmain peatlands have been modest sinks of organic C compared to those of Alaska, western Canada and western Siberia, although differences in calculation methods hamper direct comparisons. Considering within-peatland dynamics, maximum total C sequestration coincided with a period of slowing down in both lateral expansion and vertical accumulation. Late-Holocene diminishing peatland C sink functions have been attributed to autogenic as well as allogenic factors. Height-induced surface drying and/or Neoglacial cooling effects may have forced the slowing down of C sequestration in the studied bogs. Results further show that, in order to obtain an accurate quantification of past C sequestration, reconstructions of peatland expansion are essential.

Key words: carbon accumulation, chronology, peat bog, boreal, LORCA, northeastern Canada

1. Introduction

At a local scale, boreal peatlands generally act as small sinks of carbon dioxide (CO_2) and large sources of methane (CH_4), while on a global scale they constitute a net sink of organic carbon (C) [*Roulet*, 2000]. Greenhouse gas fluxes between peatlands and the atmosphere have the potential to influence climate radiative forcing on millenial timescales [*Frolking and Roulet*, 2007] and thus peatland C dynamics are of interest considering their feedback on atmospheric global warming. Peatland influence on atmospheric composition is illustrated by the fact that global Holocene trends in peatland initiation and expansion are linked with atmospheric CO_2 and CH_4 concentration [*Korhola et al.*, 2010; *MacDonald et al.*, 2006].

Carbon accumulates as organic detritus under waterlogged conditions when the rate of biomass production exceeds its decomposition [*Turunen et al.*, 2002], with both processes showing variations on seasonal to millenial timescales [*Beilman et al.*, 2009; *Borren et al.*, 2004; *Bubier et al.*, 2003; *Dorrepaal et al.*, 2009; *Schimel et al.*, 2001]. The global northern peatland store has been accumulated notably for 12 000-8000 years [*MacDonald et al.*, 2006], resulting in a C stock of ~547 Pg covering an area of 3-4 × 10^6 km^2 [*Yu et al.*, 2010].

Global peat accumulation patterns vary with latitude [*Beilman et al.*, 2009], permafrost presence [*Turetsky et al.*, 2007; *Beilman et al.*, 2009], precipitation [*Gorham et al.*, 2003], continentality [*Tolonen and Turunen*, 1996], peatland age and depth [*Belyea and Clymo*, 2001; *Clymo*, 1984], fire events [*Pitkänen et al.*, 1999; *Turetsky et al.*, 2002], peatland type [*Turunen et al.*, 2002] and surface microtopography presence [*Eppinga et al.*, 2009; *Malmer* *and Wallén*, 1999; *Swanson*, 2007]. Hence, the characterization of regions with important peatland cover is essential to accurately quantify the global peat C store and estimate future greenhouse gas budgets.

Considering accumulation gradients at a local scale, autogenic changes in hydrology and differential peat growth can be linked to changes in peatland surface topography [*Belyea and Baird*, 2006], while spatial variations in the C balance on short and long timescales may be considerable [*Malmer and Wallén*, 1999; *Waddington and Roulet*, 1999]. In topographic depressions with a uniform shape, peat accumulation is typically initiated in the lowest section which implies that subsequent peat accumulates both vertically and laterally. Hence, the age of peat inception generally decreases toward the basin margins and thicker peat deposits are located near the center of the basin. In most peatland types, margins differ hydrologically and botanically from the central parts. Margins are often characterized by a denser tree and shrub cover as water tables are lower and more sensitive to fluctuations [*Bauer et al.*, 2009; *Bubier*, 1991].

Current variable estimations of the northern peatland C stock are the result of differing assumptions on global average peat depth [*Gorham*, 1991] and bulk density [*Turunen et al.*, 2002] or inaccurate spatial inventories and volume models [*Beilman et al.*, 2008; *Vitt et al.*, 2000]. Apparent rates of C accumulation (expressed in g m^{-2} yr^{-1}) calculated from a single, central core within a peatland may result in estimations of total C sequestration that inadequately represent the entire system [*Turunen et al.*, 2002]. One reason for central coring sites might be a preference for long historical records of peat development. However, this record might poorly represent the entire ecosystem as spatial variability can not be quantified. Poor temporal correlation between vertical and lateral peat accumulation within a single bog has been found repeatedly [e.g. *Korhola*, 1994; *Korhola et al.*, 2010]. Hence, more accurate C accumulation rates can be obtained using patterns from various downcore sections taking account of variations in depth and minimal ages of peat inception, especially if local basin topography is complex.

Spatial peat accumulation reconstructions and quantifications of C sequestration have been performed in Scandinavia [*Korhola*, 1994; *Korhola et al.*, 1996; *Mäkilä*, 1997; *Mäkilä and Moisanen*, 2007], Scotland [*Chapman et al.*, 2009], western Canada [*Bauer et al.*, 2003; *Beilman et al.*, 2008] and western Siberia [*Borren and Bleuten*, 2006; *Sheng et al.*, 2004; *Turunen et al.*, 2001]. Despite an important coverage on the Quebec territory [9-12%, *Payette and Rochefort*, 2001], C sequestration data from boreal peatlands east of Hudson Bay and James Bay is limited. Presently, C accumulation rates have been quantified by *Loisel and Garneau* [2010] from four one-meter long cores collected in two of the Eastmain peatlands presented here. Peat and C accumulation rates have also been determined from cool-continental and maritime bogs in the southern regions of eastern Canada [*Turunen et al.*, 2004] as well as from ombrotrophic peatlands in the mixedwood forest biome [*Gorham et al.*, 2003; *Turunen et al.*, 2004]. *Beaulieu-Audy et al.* [2009] calculated vertical peat accumulation rates in boreal peatlands from the La Grande Rivière region, northern Quebec, but did not provide quantitative data on the rate of C accumulation. In this paper we present reconstructions of peat accumulation and long-term C sequestration patterns from three pristine ombrotrophic peatlands in the Eastmain region of northeastern Canada (51º50’-52º20’N/75º00’-76º00’W). The main objective is to quantify regional Holocene C accumulation in terms of C mass, density and accumulation rates. A secondary objective consists in increasing the knowledge on C sequestration variability within and between peatlands from the same region and to compare our results with data from western North America and Eurasia.

Previous research on lateral and vertical peat accumulation has shown rapid lateral expansion of peatland ecosystems in the early stages, with a slowdown in the course of their development [*Mäkilä*, 1997; *Mäkilä and Moisanen*, 2007], although smaller-scale variations in peatland expansion rates may be primarily controlled by basin topography [*Korhola*, 1994]. In accordance, we expect slowing down of peatland expansion in the Eastmain region toward the late-Holocene. However, global tendencies in vertical peat accumulation may be less uniform. Peatlands in oceanic settings typically show concave age-depth models, resulting principally from the effects of constant productivity and continuous C loss in the catotelm as indicated by *Clymo* [1984]. In contrast, continental bogs often show convex age-depth models [*Kuhry and Vitt*, 1996; *Turunen et al.*, 2001], implying long-term slowdown of accumulation during peatland development [*Yu et al.*, 2003]. This trend may be driven by autogenic or allogenic influence or a combination of both [*Belyea and Malmer*, 2004]. As the Eastmain region has neither an oceanic nor a strictly continental setting, we hypothesize that the studied peatlands show approximate linear vertical accumulation.

Holocene C accumulation rates of two boreal peatlands located ~400 km south of our study region were quantified at approximately 21.9 and 29.4 g m^{-2} yr^{-1} [*Gorham et al.*, 2003]. As global C sequestration rate optima are associated with a mean annual temperature (MAT) of around 0ºC [*Beilman et al.*, 2009] or 0ºC to 2.5ºC [*Yu et al.*, 2009], potential rates are likely to decrease northward of ~50ºN in Quebec. The Salym-Yugan peatland complex in western Siberia is subjected to MAT and mean annual precipitation (MAP) comparable to the Eastmain region; showing a mean rate of 17.2 g m^{-2} yr^{-1} [*Turunen et al.*, 2001]. Based on these data, we hypothesize that Holocene C accumulation rates of the Eastmain region peatlands might average 15–25 g m^{-2} yr^{-1}.

2. Study region

The three studied peatlands Lac Le Caron (LLC), Mosaik (MOS) and Sterne (STE) are located in the Eastmain river watershed in the boreal forest region of the James Bay lowlands of Quebec (Fig. 1). Regional MAT is -2.1 ± 0.2°C (January: -22.0 ± 0.5ºC; July: 14.6 ± 0.2ºC) and MAP is 735 ± 12 mm, of which about one third falls as snow [*Hutchinson et al.*, 2009]. The region is characterized by Proterozoic bedrock and glacial and postglacial landforms as drumlins and eskers. Deglaciation occurred between 8500 and 7900 cal BP [*Dyke et al.*, 2003] and was followed by the Tyrrell Sea invasion that caused the deposition of marine and deltaic sediments in the western part of the territory. The regional upland vegetation corresponds to the limit of the *Picea mariana*-feathermoss and *Picea mariana*-lichen bioclimatic region [*Saucier et al.*, 1998]. Peatlands cover ~7% of the Eastmain region varying from treed bogs to wet fens [*Grenier et al.*, 2008]. The studied peatlands are classified as pristine (eccentric) raised bogs characterized by a well-developed hummock-hollow patterned surface with deep pools (~2 m) in their central sections [*Loisel and Garneau*, 2010]. Peat accumulation started by paludification as peat types identified at the base of the cores did not reveal past infilling ponds.

Lac Le Caron bog (LLC) (52º17'15"N/75º50'21"W; 2.24 km^2 area) is located in the northwestern part of the region (Fig. 1). The western part of the basin is bordered by a steep, ~40 m-high escarpment while the eastern limit is relatively flat with a stream flowing southward. The center of LLC bog is treeless with wet hollows and large pools. Sedges are more abundant than in the surrounding ribbed section. The bog margins are forested and dominated by *Picea mariana*. A fen characterized by a near-surface water depth is present next to the pool sections and sparse *Larix laricina* grow occasionally on lawns. Drainage is directed toward the eastern section of the system. The mineral basin sediments are highly variable from fine sand to silt.

Mosaik bog (MOS) (51º58’55”N/75º24’06”W; 2.67 km^2 area) is located 45 km southeast of LLC bog (Fig. 1), where topography is less pronounced. The center of this peatland is characterized by an important presence of wet hollows and numerous large pools with outcrops present in the northern section. Bog margins are colonized by *Picea mariana* while the southwestern part was affected by a local fire in 1997 and is characterized by sparse *Pinus banksiana* Lamb. Multidirectional hummock-hollow patterns may indicate a complex pattern of drainage. Mineral sediments range from coarse to fine sand with pebbles or (bed)rock.

Finally, Sterne bog (STE) (52º02’37”N/75º10’23”W; 1.72 km^2) is located 17 km northeast of MOS bog (Fig. 1). As MOS bog, its central section is very wet with many large pools. The eastern part has an indistinct forest-bog transition. In the southwestern part, a small stream separates the bog from a large poor fen. The mineral basin of STE bog is characterized by poorly sorted coarse and fine sands and a frequent presence of pebbles or (bed)rock.

Each of the studied peatlands shows a forested border of varying width. This ecotonal limit shows both abrupt and indistinct transitions. On the open peatlands, trees of *Picea mariana* are sparsely distributed on hummocks. Ericaceous shrubs such as *Chamaedaphne calyculata*, *Kalmia angustifolia*, *Rhododendron groenlandicum* and *Andromeda glaucophylla* are distributed following a moisture gradient. Cyperaceae are abundant in lawns and hollows: *Eriophorum vaginatum*, *Trichophorum cespitosum* and *Carex* spp. Dominant bryophytes are *Sphagnum fuscum* and *Sphagnum angustifolium* on hummocks, *Sphagnum russowii* and *Sphagnum magellanicum* on lawns, whereas *Sphagnum cuspidatum*, *Sphagnum fallax* and *Sphagnum majus* are frequent in wet hollows.

3. Material and methods

3.1. General approach

Quantifying C accumulation in a peatland implies the integration of areal extent, variability of deposit thickness and related C density. A chronological approach integrating both age and peat thickness was adopted to reconstruct rates of C sequestration through time. The accuracy of the reconstruction depends directly on the spatial uniformity of the age-depth relation. Models of peat cover thickness were created from field probing measurements and Ground-Penetrating Radar (GPR) analyses. Added to these models were radiocarbon datings from multiple cores sampled in different sections of the peatland resulting in age-depth relationships. Afterward, peatland development was divided into 250-year time slices that were linked to peat depth values. The combination of peat depths and the spatial cover thickness model resulted in a definite volume of peat accumulated during each time slice. This volume was then converted in mass of organic C using bulk density and loss-on-ignition (LOI) data, resulting in a quantification of the C flux. The total mass of C was represented by the sum of C fluxes for all time slices.

3.2. Peat depth models

The areal extent of the studied peatlands was determined by aerial photo interpretation and field validation. Peatland surface altitude was obtained by a Trimble 5800/5700 Differential Global Positioning System (DGPS) along a number of transects per peatland during the summer of 2006. Peat thickness was determined by a combination of manual probing with an Oakfield soil sampler and GPR analyses. Survey points were located along grids (probing) or transects (GPR) localized using DGPS (Fig. 1). At each sampling point, the composition of underlying mineral material was described. Manual probing was realized at

100- and 200-m intervals. GPR measurements were performed with a PulseEKKO (Sensors & Software Inc.) at 0.25 m to 1 m resolution using both 100 MHz and 200 MHz antennae during a winter campaign in 2007 and the summer of 2008. Time delay between electromagnetic wave emission and reception was converted to peat cover thickness using a mean peat velocity, determined by common mid-point analysis [*Neal*, 2004] and target-to-depth technique [*Rosa et al.*, 2009]. Data were processed with basic editing (Dewow filter, AGC gain, FK migration) [*Jol and Bristow*, 2003] with Reflexw software [*Sandmeier*, 2005] in order to identify the organic-mineral contact. Data were compiled to create peat thickness models using ArcGIS 9.3. Peat thickness models were created using ordinary kriging interpolation using a spherical model to fit to the variograms. Model selection was based on the lowest mean standardized error obtained by cross-validation, as in most cases mean root-mean-square errors were not significantly different (F test, $P = 0.05$). Cross sections showing present-day peatland surface and mineral basin topography were created to obtain an image of peatland geometry. As the cross-section was supposed to deliver a global image, surface topography data was smoothed by a locally weighted least squared error method with 5% smoothing factor using Kaleidagraph 3.6.

3.3. Age-depth relationships and peat volume accumulated per period

Multiple cores were extracted from each peatland during field campaigns in August 2006 and July 2007 (Fig. 1). Based on manual probing results, a core was sampled where peat thickness was found to be maximum. Although referred to as central core, its position did not correspond to the geographic center of the peatland because of the complexity of the basin topography. In addition, five to six shallower lateral cores, located along the margins, were extracted from each peatland. Each lateral core was sampled in a different quadrant of the peatland to cover spatial variability. All profiles were collected using a Box corer (10×10 cm width) for the top 1 m and Russian peat samplers (4.5-cm or 7.5-cm diameter) for the deeper, compacted peat. Cores were extracted from surface lawn microforms as these are likely to be more sensitive to environmental change than hummocks [*Nordbakken*, 1996; *Rydin*, 1993]. Monolith lengths ranged from 64 to 483 cm with variability within and among peatlands. Cores were wrapped in plastic and covered by PVC tubes before storage at 4ºC until analysis. In the laboratory, cores were cut into 1-cm thick slices and subsampled for analysis. Five cores per peatland were investigated in order to reconstruct peat-forming vegetation assemblages [*Troels-Smith*, 1955]. To obtain reliable chronologies, a total of 91 subsamples were radiocarbon dated at the Keck-CCAMS facility (Irvine, USA) and Beta Analytic Inc. (Miami, USA). For each peatland, chronologies of the deep core and two lateral cores were based on numerous datings, whereas of the remaining lateral cores only basal peat was dated (Table 1). If present, *Sphagnum* stems were dated because these yield most reliable ^{14}C dates [*Nilsson et al.*, 2001]. Other levels were dated using leaf or seed fragments of Ericaceae and Cyperaceae, and in some cases charcoal fragments. Datings were calibrated using the IntCal04 calibration curve [*Reimer et al.*, 2004] within the Bchron software package [*Haslett and Parnell*, 2008]. All ages are expressed as calendar years before present (BP = before AD 1950). For each peatland, Bchron output ages were converted to an age-depth model using JMP 7.0. The surface was assigned either -56 or -57 cal BP (i.e. 56 years after reference year AD 1950), as the peat cores were sampled in AD 2006 and 2007. Only the permanently waterlogged catotelm peat was modelled, as decay is important in the (temporally) aerated acrotelm resulting in differential accumulation dynamics. Both linear and polynomial models were tested, as catotelm peat accumulation rarely conforms to a simple linear relation between age and depth [*Blaauw and Christen*, 2005]. The original model showed heteroscedasticity, hence a transformation was applied by modelling the square root of the original dependent variable “depth”. Parameters were tested and the distribution of residuals was studied for each model. After selection of the appropriate age-depth model, the peat sequence history was divided into 250-year time slices. As the acrotelm was excluded, the upper limit of the model was defined at 250 cal BP. Concerning the base of the peat cover, an additional assumption had to be made. GPR measurements performed after coring detected sections of the peatland containing peat deposits of which the thickness exceeded the length of the central cores. As a result, the deepest sections of the peatland are not covered by the age-depth model. As extrapolation of age was assumed to be unreliable due to nonlinearity of age-depth relationships, the adopted chronologies only cover the range corresponding to that of the central core. Levels that exceeded this depth were assigned an age range of “*x*-8000 cal BP”, with *x* representing the age of the oldest dated sample for each peatland. The upper and lower limits of each time slice were linked to a depth determined from the corresponding age-depth model. These depths were integrated into the peat thickness model to estimate the volume of accumulated peat per time slice. Volumes were calculated using the 3D Analyst toolbox in ArcGIS 9.3.

3.4. Peat organic C content and density

The organic C content of peat was calculated using data from LOI analysis and mean C content of organic matter (OM). The product of bulk density and LOI analyses determined the density of OM [*Dean*, 1974]. Dry bulk density was measured from consecutive 1 cm^3 subsamples after drying in an oven for 16 hours at 105ºC. Subsamples were combusted at 550ºC for 3.5 hours to determine LOI [*Heiri et al.*, 2001] and the resulting OM density was converted to C mass per unit volume (C density) assuming a constant mean peat C content of 50% relative to OM. Subsequently, mean C density values for each peatland were applied to the undecomposed, upper peat (younger than 250 cal BP) and decomposed, deeper peat. The boundary between upper and deeper peat corresponded closely to the level of C density culmination. Considering the deep peat, C density showed high variability both within cores and peatlands. As a uniform relationship between peat depth and C density was absent within the deep peat, we applied a mean C density for each peatland individually. This mean density for deep peat was based on subsamples of all cores within each peatland.

3.5. Peat C stocks and C accumulation rates per period

The amount of C added per time slice was calculated by multiplying the volume of peat by the mean C density. The total C mass of each peatland was obtained by the sum of C accumulation values for all time slices. Holocene C accumulation rates were calculated by dividing the mass of C accumulated (g) by the mean period of accumulation (yr) for a constant surface area (m^2) [*Clymo et al.*, 1998]. This mean period of accumulation was based on the peat depth distribution and the peatland-specific age-depth model. In addition, recent apparent rates of C accumulation [sensu *Tolonen and Turunen*, 1996] were calculated for the upper peat layer (i.e. the most recent time slice).

4. Results

4.1. Basin and surface topography

The stratigraphic mineral-organic transition was generally sharp in each peatland, identified through GPR images, LOI results as well as from probing. Peat thickness values from manual probing and GPR at identical locations were highly linearly correlated

($r^2 = 0.90$; n = 30) showing the accuracy of both methods. Applied mean velocity was relatively high at 0.040 and 0.046 m ns^{-1} [*Hänninen*, 1992; *Leopold and Volkel*, 2003; *Rosa et al.*, 2009] possibly due to winter conditions and low water temperatures.

The basin topography shows high small-scale variability possibly associated with local presence of bedrock or boulders (Fig. 2). Especially in LLC bog, local depressions are present, indicating that the peatland may have been formed by the fusion of numerous mesotopes [sensu *Charman*, 2002].

Present-day surface topography shows variation in altitude of 2 to 8 m within the peatlands (Fig. 2). LLC (sloping southeastward at ~5 m km^{-1}) and STE (sloping westward at ~3 m km^{-1}) have most pronounced gradients, whereas MOS bog has a flatter surface. However, MOS and STE have more typical raised bog shapes with an elevated center, while LLC bog does not show the typical dome morphology.

4.2. Peat cover thickness

Maximum peat thickness is 531 cm in LLC bog as obtained by probing, showing that the deepest core (LLC_C), measuring 483 cm, was effectively sampled within the thickest peat deposits. However, GPR analyses in MOS and STE bogs show maximum peat deposit thickness of 385 cm and 412 cm, whereas their central cores measured 297 cm (MOS_C) and 286 cm (STE_C). Generally, the thickest peat deposits are located off-center within each peatland, influenced by local basin topography (Fig. 2). Because the dated peat cores did not cover the complete range of peat thickness, the age-depth models of MOS and STE bogs are slightly biased toward the shallower peat deposits and do not as well represent basal peat accumulation as does the LLC bog chronology.

4.3. Radiocarbon dating and age-depth models

Basal ages of the different lateral and central cores range from 1211 to 7520 cal BP (Table 1). The basal ages of the three studied peatlands are 7520 cal BP for LLC bog, 7340 cal BP for MOS bog and 7127 cal BP for STE bog and confirm that peat inception started early after deglaciation in the region [*Dyke et al.*, 2003]. For LLC bog, a second-degree polynomial model ($r^2 = 0.86$) with significant parameters ($P < 0.05$) best fitted the relationship between the square-root of depth and age, based on the distribution of the residuals (Fig. 3). Although age-depth relationships were modelled with a transformed "depth" variable, the models are shown with linear axes. MOS ($r^2 = 0.75$) and STE ($r^2 = 0.69$) bogs were best represented by a significant linear model (both $P < 0.0001$).

The convex model representation of each peatland shows vertical peat accumulation slowdown in the course of its development. The most important change in accumulation rate occurred in LLC bog, declining from 0.103 cm yr^{-1} between 7520 and 6520 cal BP to 0.016 cm yr^{-1} between 1250 and 250 cal BP. MOS bog accumulation slowed down from 0.036 to 0.018 cm yr^{-1} whereas STE bog rates showed a decline from 0.034 to 0.019 cm yr^{-1} both from the first millenium to the 1250-250 cal BP period. Highest similarities between age-depth models are found toward the late-Holocene.

4.4. C density and mass per unit area

The mean C density from all peat samples is 44 kg m^{-3} (SE = 0.0003; n = 3606) with slight variations among peatlands (Table 2). C density was lowest in the living moss layer and generally increased downward until a peak around 250 cal BP (Fig. 4). C density did not show a consistent increasing trend toward deeper peat in the anaerobic section (Fig. 4), indicating that vegetation type-related humification might be as important as the age of peat formation. Instead, temporal variations in microforms and peat-forming vegetation may explain the variations in the deeper peat C density data. Stratigraphic analysis [*Troels-Smith*, 1955] showed variations in peat-forming vegetation within each core with alternance of *Sphagnum*, herbaceous and ligneous peat, which may be due to internal microform dynamics or external forcing, or both (Fig. 5).

Mean area-weighted C mass per unit area is 91 kg m^{-2} with a highest mean in LLC bog (Table 2). As LLC does not show the highest mean C density, its higher C mass per unit area primarily results from a higher mean peat thickness (Table 2). Thus, without considering the present-day surface area of the studied Eastmain peatlands, LLC bog has been the most important sink of organic C throughout the Holocene.

4.5. Peatland area and C accumulation reconstructions

Lateral peatland expansion rates were high in the early stages of development (Fig. 6). Early rapid peatland development was followed by a gradual decline in lateral accumulation rates that started as early as 6000 cal BP in the three peatlands. Although initial paludification is suspected to have a maximum age of 8000 cal BP, the combination of age-depth and spatial peat thickness modelling implies that 50% of the present peatland area was covered by peat deposits around 5500 cal BP.

Ecosystem-scale C flux reconstructions show similar trends for each peatland (Fig. 7), with an increase during the first millennia, peaking during the mid-Holocene, followed by a decline toward the late-Holocene. The most recent time-slice (0-250 cal BP), which includes the acrotelm, shows high values as decay is incomplete. Despite the comparable tendencies between the three peatlands, variations in timing are visible (Fig. 7). In LLC bog, C fluxes show greater variations in time, culminating between 5250 and 5000 cal BP, with an equivalent rate of 41 400 kg yr^{-1}. In MOS and STE bogs, C accumulation appears to have been more stable, with highest fluxes of 27 000 kg yr^{-1} and 18 000 kg yr^{-1} between 3750 and 3500 cal BP, respectively. Lateral expansion has been most important in the early stages of peat bog development, while vertical accumulation of peat slowed down during the entire history of the peatlands (Fig. 3 and 6). However, the periods with maximum ecosystem C flux (5250-5000 cal BP in LLC bog and 3750-3500 cal BP in MOS and STE bogs) correspond to the optima in the balance of both directions of accumulation. Hence, although counterintuitive, maximum ecosystem C fluxes coincided with periods of diminishing lateral and vertical accumulation rates in each of the ecosystems.

Although MOS bog presently covers the largest area, LLC bog has accumulated the highest amount of C: 242×10^6 kg, compared to 217×10^6 kg C for MOS bog. The smaller STE bog presently contains 149×10^6 kg C (Table 2). Taking into account peatland surface area and mean age of peat initiation, Holocene C accumulation rates were 18.9, 14.4 and 15.2 g m^{-2} yr^{-1}, for LLC, MOS and STE bogs respectively, corresponding to an area-weighted regional mean (±SE) of 16.2 g m^{-2} yr^{-1} (±1.4). Mean C accumulation rate (±SE) of the most recent time slice is 56.4 g m^{-2} yr^{-1} (±1.7); values for peatlands individually are shown in Table 2.

Results from peat composition analysis show that ombrotrophication occurred rapidly after initial peat accumulation in a number of cores with some sections showing delayed or very recent shifts to ombrotrophic conditions, e.g. MOS_L1 (~160 cal BP) and STE_L4 (~220 cal BP) (Fig. 5). Nevertheless, no significant differences in mean age of ombrotrophication are discernible between ecosystems ($F = 0.91$; $P = 0.45$).

5. Discussion

5.1. *Age-depth modelling and C accumulation patterns*

The age-depth models presented are based on chronologies from cores that covered the variability in deposit thickness of each peatland. The age-depth model of LLC bog represents well the range of peat cover thicknesses and has a high r^2 of 0.86. However, MOS and STE bog chronologies are slightly biased toward younger peat deposits as the obtained chronology did not cover the deepest peat. In addition, their respective age-depth models show lower r^2 at 0.75 and 0.69 which implies that the relationship between age and depth is more variable within these peatlands. For these reasons, the older sections of the MOS and STE age-depth model need to be interpreted with caution. It is probable that a central core within the deepest section of these peatlands results in a more convex age-depth model, revealing C accumulation patterns that would more closely resemble those of LLC bog.

The presented reconstructions of the three peatlands show that lateral expansion has been important in their early development. In addition, net vertical accumulation rates have diminished continuously, causing a slowdown of C accumulation rates. Although trends are comparable, MOS and STE bogs showed less variable rates of vertical accumulation than LLC bog, which resulted in a minor decrease in C accumulation rates in the late-Holocene. Generally, peatland hydrology and microhabitat patterns are influenced by both internal dynamics (autogenic factors) and external forcing (allogenic factors) on varying timescales [*Belyea and Baird*, 2006; *Payette*, 1988], which will be discussed here relative to the observed patterns.

5.2. *Autogenic factors*

Internal processes may to some extent explain different tendencies in peatland development. Of all types of autogenic change, ombrotrophication may be the most important considering peatland C sequestration [*Charman*, 2002]. Typical net C accumulation rates differ between fens and bogs [*Turunen et al.*, 2002; *Yu*, 2006] and thus hydroseral succession may well result in a step-like change in C cycling [*Belyea*, 2009]. However, stratigraphic analyses have not shown distinct differences in the timing of ombrotrophication between the studied peatlands. In contrast, *Loisel and Garneau* [2010] reported more recent ombrotrophication in MOS bog in comparison with LLC bog. However, only one section of each peatland was considered in their study.

The uniform highly sloping surface (~5 m km^{-1}) of LLC bog (Fig. 2) may have resulted in a more effective lateral drainage through subsurface flow than in MOS and STE bogs. This could have resulted in a more frequent peat surface drying since slope development. An effective drainage in LLC bog is also visible through the minor presence of wet hollows and large ponds relative to MOS and STE bogs (Fig. 1).

Lateral expansion of the peatlands is shown to have been an important factor on C accumulation. Although net vertical accumulation rates at the ecosystem scale have diminished during the entire Holocene, maximum C accumulation rates were attained as late as the mid-Holocene, as basin geomorphological constraints apparently induced a delay in the culmination of ecosystem C sequestration rates in the three peatlands. Lateral expansion of peatlands has been reported to be primarily influenced by local factors as topography [*Bauer et al.*, 2003; *Korhola*, 1994; *Mäkilä and Moisanen*, 2007]. Therefore, site-typical patterns of lateral expansion may cause different temporal patterns of total C accumulation between peatlands. The local topography near LLC bog is complex (Fig. 2), with a steep outcrop at its western limit and a neighbouring stream in the eastern part. Hence, lateral peatland expansion may have been inhibited during development and this confinement could partially explain the decline in C accumulation. *Belyea and Clymo* [2001] showed that, in peatlands that are constrained in their development by mineral basin topography, the potential for water storage in the catotelm and thus peat accumulation decreases over time.

In addition to the spatial complexity of the studied peatlands, a nonlinear feedback to either allogenic or autogenic change may be present. The ecosystem's reaction to environmental change depends not only on the strength of the forcing but also on the height of the threshold value [*Belyea*, 2009]. In this context, the resilience of peatland hydrology and vegetation might be of major importance when evaluating the reaction of the ecosystem to environmental change. As LLC bog surface topography is sloping uniformly, while MOS and STE bogs have more lens-shaped cross-sections, surface runoff patterns are likely to differ. Differential resilience between the Eastmain region peatlands might be another explanation for asynchronous shifts in C accumulation.

5.3. Allogenic factors

The gradual slowdown of net long-term C accumulation in LLC bog from 5000 to 250 cal BP and from 3500 to 250 cal BP in MOS and STE bogs (Fig. 7) corresponds to declining C sequestration rates observed in other continental peatlands in North America [*Beaulieu-Audy et al.*, 2009; *Vardy et al.*, 2000; *Vitt et al.*, 2000; *Yu*, 2006; *Zoltai*, 1995]. This common trend may indicate the presence of an external factor such as climate change that could have mediated autogenic development. Holocene temperature reconstructions show the presence of cooling starting between 4000 and 3000 cal BP for both the entire North American continent and northern Quebec [*Viau et al.*, 2006]. *Beaulieu-Audy et al.* [2009] found slowdown of peat accumulation in two ombrotrophic peatlands north of the Eastmain region from 4500 to 1500 cal BP, whereas peatland permafrost aggradation was reported starting around 3500 cal BP [*Bhiry et al.*, 2007] in the forest-tundra biome. A colder climate has also been responsible for a decline in forest productivity after 4650 cal BP about 150 km north of this study region [*Arseneault and Sirois*, 2004]. Lower primary productivity caused by a prolonged period of peatland surface frost and shorter growing seasons may have suppressed C accumulation rates [sensu *Mauquoy et al.*, 2002]. Slowdown of C sequestration in fens and bogs has also been reported from continental western Canada starting between 4000 and 3000 cal BP, in some cases linked to permafrost development [*Vardy et al.*, 2000; *Vitt et al.*, 2000; *Yu*, 2006; *Zoltai*, 1995].

As the Eastmain peatlands are at maximum 53 km apart, a spatially uniform climate regime can be assumed. The observed differences in timing and intensity of C accumulation trends between LLC bog and MOS and STE bogs seem inconsistent with the premise of a high sensitivity of peat C dynamics to Holocene hydroclimatic variations. Differences in past vegetation assemblages might explain different C sequestration patterns, yet analyses to this respect did not indicate a distinct difference in ombrotrophication between peatlands (Fig. 5). Vegetation shifts have been important throughout most of the peat cores, being as important as vegetation variability within and among peatlands (Fig. 5), which might imply a strong local hydrological control on vegetation.

Besides, isostatic uplift after the retreat of the Wisconsian ice sheet has been extremely high at around 220 m in the present-day James Bay region [*Andrews and Peltier*, 1989]. As the total uplift shows a descending northwest-southeast gradient and the general drainage in the Eastmain region is northwestward, this differential uplift might have resulted in a decreasing slope of the Eastmain watershed region. Due to differential uplift, LLC bog may have risen 10 to 20 m more than MOS and STE bogs since 7000 cal BP. Such a difference may have influenced regional drainage through river incision. If incising rivers form a base level for peatland hydrology, this may result in a drawdown of the regional peatland water table mound. This mechanism has been proposed to explain variations in patterns of peatland development on the low-relief, southwestern Hudson Bay lowlands [*Glaser et al.*, 2004]. The differential uplift within the region studied by *Glaser et al.* [2004] is on the order of 40 m over the last 7000 years, with highest uplift occurring in the northeastern section. If the same dynamics were applicable in the Eastmain region, LLC bog, which could have suffered most from increases in regional drainage potential, would have registered most important bog surface drying and hence a slowing down of C accumulation. However, we do not have evidence of river incision at the eastern limit of LLC bog.

Stratigraphic analyses showed the presence of macroscopic charcoal fragments, indicating possible local burning events. Recurrent fires have a potential to affect long-term rates of accumulation in boreal peatlands, with emissions estimated at 2.2 to 2.5 kg C m^{-2} per event [*Pitkänen et al.*, 1999; *Turetsky and Wieder*, 2001]. Although forest fires may not frequently affect wet, open peatland ecosystems [*Hellberg et al.*, 2004], recent observations in the Eastmain region showed that fires may well burn central sections dominated by wet hollows after extreme drought. As the LLC bog is bordered by a steep ridge in the western part and the regional dominant fire direction is northwest-southeast [*Bergeron et al.*, 2004], LLC bog might have been less exposed to frequent fire events than MOS and STE bogs. However, as macroscopic charcoal fragments may easily be transported over several hundreds of meters [*Peters and Higuera*, 2007], we can not yet provide estimates of past frequencies of peatland burning in the Eastmain region. Peatland fire history linked to long-term C dynamics will be reconstructed for a future publication.

5.4. C accumulation rates

The mean basin C sequestration rate of the three peatlands is 16.2 g m^{-2} yr^{-1}. One should keep in mind that these rates are apparent and thus differ from net ecosystem production as millennia of deep decomposition have passed. This value is on the lower side of our hypothesized range of 15-25 g m^{-2} yr^{-1} that was based uniquely on present-day climate conditions (MAT and MAP). Thus, the difference between the hypothesized and the reconstructed values may be explained by differences in past climate regimes, climate variables other than MAT and MAP, disturbance regimes and geological (tectonic) and geomorphological (substrate) factors. In eastern Canada, late-Holocene climate regimes are likely to have been colder than present-day, possibly explaining the relatively low C sequestration values. In addition, peatland development was delayed by late deglaciation. Hence, a relatively large part of the total Eastmain peatland C stock was sequestered during the less favourable Neoglacial conditions, resulting in suppressed mean Holocene C sequestration rates. These C accumulation rates are lower than the reported global northern averages of 24.1 g m^{-2} yr^{-1} [*Lavoie et al.*, 2005] and 18.6 g m^{-2} yr^{-1} [*Yu et al.*, 2009]. However, averages from single cores are likely to overestimate rates at the ecosystem scale as presented here; therefore direct comparisons may be hazardous. The obtained mean recent C accumulation rate of 56.4 g m^{-2} yr^{-1}, representing the recentmost 306 years of accumulation, is comparable to the mean ~150-year accumulation rate of eastern Canadian bogs of 73 g m^{-2} yr^{-1} [*Turunen et al.*, 2004] and 74 and 84 g m^{-2} yr^{-1} for other cores from LLC and MOS bogs [*Loisel and Garneau*, 2010]. The lower values obtained in this study may be the result of the longer period considered for recent C accumulation rate calculation, as these values generally diminish with depth due to a higher proportion of decomposed peat [*Turunen et al.*, 2004].

At the global scale, highest long-term C accumulation rates may coincide with climates with MAT of 0-2.5ºC and MAP of 400-550 mm [*Yu et al.*, 2009]. The Eastmain region peatlands are close to the wet/cold limit of northern peatlands within the northern peatland distribution of *Yu et al.* [2009]. To correctly interpret differing C sequestration patterns in relation to climate, the seasonal precipitation distribution and temperature patterns should be taken into account. The effect of precipitation on boreal peatland hydrology may vary depending on the precipitation type (i.e. rain or snow) [*Charman*, 2007], whereas warm summers but cold winters are likely to be favourable to C sequestration [*Jones and Yu*, 2010]. In addition, it should be noted that the link between climate regime and temporal shifts in C sequestration is nonlinear. *Gorham et al.* [2003] stated that high rates of peat C accumulation are found in North American and Siberian dry continental regions. However, despite the good correlation between relatively dry climate and rapidly accumulating peatlands, dry shifts in climate will not in all cases cause increasing C accumulation rates. The reaction of a peatland to environmental change is mediated by microtopographic dynamics (e.g. bistability and spatial self-organization) [*Eppinga et al.*, 2009] showing an underestimated complexity of these systems. Thus, the direction of the ecosystem's pathway may depend on the present phytoecological and hydrological state relative to the climate shift, the rapidity of the forcing and the height of the threshold.

5.5. C density and mass per unit area

The mean C density from the studied peatlands of 44 kg m^{-3} is close to estimates from other regions. *Vitt et al.* [2000] obtained variable C densities depending on peat type: 49 kg m^{-3} for open fens and bogs and 55 kg m^{-3} for wooded and shrubby fens. *Beilman et al.* [2008] reported a mean of 93 kg OM m^{-3} in the boreal Mackenzie River Basin of northwestern Canada, which represents approximately 47 kg C m^{-3}. In Alaskan bogs with C sequestration rates similar to those of the Eastmain peatlands, mean C densities of 42–47 kg m^{-3} were obtained compared to 35-37 kg C m^{-3} south of the Eastmain region [*Gorham et al.*, 2003]. In western Siberia, a mean ombrotrophic peat C density of 32 kg m^{-3} was reported [*Bleuten and Lapshina*, 2001]. Assuming 50% of C in OM, 46 kg m^{-3} was obtained by *Turunen et al.* [2001] for west-Siberian peatlands and a mean C density of 36 kg m^{-3} was found in a hummock-hollow pine bog in southeastern Finland [*Mäkilä*, 1997]. Important differences between peatlands within a region may indicate that local and short-term factors as vegetation type and hydrology may be determinant considering C density values.

Mean area-weighted C mass per unit area for the Eastmain peatlands is 91 kg m^{-2}. This value is lower than 131 kg m^{-2}, 118 kg m^{-2} and 119 kg m^{-2} obtained from peatlands in (south)western Canada [*Vitt et al.*, 2000], northwestern Canada [*Beilman et al.*, 2008] and the western Siberian lowlands [*Sheng et al.*, 2004], respectively. It is also lower than the mean 124 kg m^{-2} and 108 kg m^{-2} for the raised bog and aapa mire region in Finland [*Mäkilä and Goslar*, 2008] and 94 kg m^{-2} as an average for Scottish peatlands [*Chapman et al.*, 2009]. Comparisons between regions are hampered by methodological differences, which partially explain lower values for Eastmain region peatlands.

5.6. Future perspective on potential C sequestration

To estimate future C sequestration patterns in the Eastmain region, a detailed image of the factors driving long-term C accumulation rate decline is crucial. For now, we do not have indications that either autogenic or allogenic factors are dominant due to the complexity of these ecosystems. In case the decline can be attributed primarily to autogenic factors as a height-induced long-term drying of the surface [sensu *Yu et al.*, 2003], the C sink of the Eastmain region may continue to diminish during the centuries to come. However, if long-term Neoglacial cooling has been the principal cause, the projected important warming trend with higher precipitation in the Eastmain region [*Plummer et al.*, 2006] might reverse the trend and increase the potential for C accumulation as registered from contemporaneous measurements between 2006-2008 [*Pelletier et al.*, in review]. Considering C sequestration, there is probably a close imbrication of both autogenous and allogenous factors on various timescales that requires better understanding.

6. *Conclusion*

This paper presents the first Holocene C accumulation rates from northern Quebec boreal bogs, with a mean value of 16.2 g m^{-2} yr^{-1}. Ecosystem C flux reconstructions for the Eastmain region show declining values at the onset of the late-Holocene. This slowdown of C accumulation is principally the result of a decrease in net rate of vertical accumulation. The application of the age-depth model to the entire ecosystem results in a model for lateral expansion, showing that the increase in peatland area was probably important during the early development and that ecosystem C fluxes became high once extensive area was covered by peat between 5000 and 3000 cal BP.

Variation in timing of the onset of the decline in C accumulation rates and the intensity of the slowdown between peatlands shows the influence of site-specific factors and local ecosystem complexity, however, a less accurate age-depth model for MOS and STE bogs may have caused a bias for the early stages of accumulation. Long-term diminishing rates of C accumulation in North American peatlands may be associated with two phenomena. First, potential for peat accumulation is suspected to decrease with time in peatlands that are constrained in lateral expansion [*Belyea and Clymo*, 2001]. Second, late-Holocene cooling may well have caused changes in C sequestration rates. Changes in peatland vegetation, hydrology and fire regimes as well as the formation of permafrost since ~4000 cal BP have been reported at the continent scale [e.g. *Beaulieu-Audy et al.*, 2009; *Bhiry et al.*, 2007; *Vitt et al.*, 2000; *Zoltai*, 1995].

Lateral peatland expansion is shown to be an important factor considering C sequestration at the ecosystem scale and comparisons between cores show the complexity of peatland ecosystems. Thus, in order to obtain more accurate quantifications of past C accumulation and better understand the role of peatlands in the global C cycle, multiple cores should be considered, rather than a unique central core. To estimate the direction of C accumulation trends in the Eastmain region for the centuries to come, the principal driving mechanism needs to be identified, as the principal autogenic and allogenic factors may have a contrasting influence on long-term C accumulation.

Acknowledgments

We thank Hans Asnong, Maxime Boivin, Gabrièle Guay, Claire Lacroix, Sébastien Lacoste, Julie Loisel, Éric Rosa and Charles Vaillancourt for field assistance. Thanks to Pierre J.H. Richard (Université de Montréal) for the use of the Jacques-Rousseau laboratory for analyses. We greatly appreciate the assistance by Bertrand Fournier (UQAM) with statistical analyses. Funding was provided by Hydro-Quebec Production through the EM-1 Project *Reservoirs' net greenhouse gas emissions research project (2005-2009)*. We thank the hydroclimatological scenarios team of the Ouranos consortium for providing climate variables by manipulation of 1971-2003 NLWIS data. We appreciate the useful comments of two anonymous reviewers. Thanks to *Les Tourbeux* for discussions and inspiration.

References

Andrews, J. A., and W. R. Peltier (1989), Quaternary geodynamics in Canada, in *Quaternary geology of Canada and Greenland*, edited by R. J. Fulton, pp. 543-572, Geological Survey of Canada, no. 1.

Arseneault, D., and L. Sirois (2004), The millennial dynamics of a boreal forest stand from buried trees, *Journal of Ecology*, *92*, 490-504.

Bauer, I. E., L. D. Gignac, and D. H. Vitt (2003), Development of a peatland complex in boreal western Canada: Lateral site expansion and local variability in vegetation succession and long-term peat accumulation, *Canadian Journal of Botany*, *81*(8), 833-847.

Bauer, I. E., J. S. Bhatti, C. Swanston, R. K. Wieder, and C. M. Preston (2009), Organic matter accumulation and community change at the peatland-upland interface: Inferences from ^{14}C and ^{210}Pb dated profiles, *Ecosystems*, *12*(4), 636-653.

Beaulieu-Audy, V., M. Garneau, P. J. H. Richard, and H. Asnong (2009), Holocene palaeoecological reconstruction of three boreal peatlands in the La Grande Riviere region, Quebec, Canada, *The Holocene*, *19*(3), 459-476.

Beilman, D. W., D. H. Vitt, J. S. Bhatti, and S. Forest (2008), Peat carbon stocks in the southern Mackenzie River Basin: uncertainties revealed in a high-resolution case study, *Global Change Biology*, *14*(6), 1221-1232.

Beilman, D. W., G. M. MacDonald, L. C. Smith, and P. J. Reimer (2009), Carbon accumulation in peatlands of West Siberia over the last 2000 years, *Global Biogeochemical Cycles*, *23*(GB1012), doi:10.1029/2007GB003112.

Belyea, L. R. (2009), Nonlinear dynamics of peatlands and potential feedbacks on the climate system, in *Carbon cycling in northern peatlands*, edited by A. J. Baird, L. R. Belyea, X. Comas, A. S. Reeve and L. D. Slater, pp. 5-18, American Geophysical Union, Washington.

Belyea, L. R., and R. S. Clymo (2001), Feedback control of the rate of peat formation, *Proceedings: Biological Sciences*, *268*(1473), 1315-1321.

Belyea, L. R., and N. Malmer (2004), Carbon sequestration in peatland: patterns and mechanisms of response to climate change, *Global Change Biology*, *10*(7), 1043-1052.

Belyea, L. R., and A. J. Baird (2006), Beyond "the limits to peat bog growth": cross-scale feedback in peatland development, *Ecological Monographs*, *76*(3), 299-322.

Bergeron, Y., S. Gauthier, M. Flannigan, and V. Kafka (2004), Fire regimes at the transition between mixedwood and coniferous boreal forest in northwestern Quebec, *Ecology*, *85*(7), 1916-1932.

Bhiry, N., S. Payette, and É. C. Robert (2007), Peatland development at the arctic tree line (Québec, Canada) influenced by flooding and permafrost, *Quaternary Research*, *67*(3), 426-437.

Blaauw, M., and J. A. Christen (2005), Radiocarbon peat chronologies and environmental change, *Journal of the Royal Statistical Society. Series C: Applied Statistics* *54*(4), 805-816.

Bleuten, W., and E. D. Lapshina (2001), *Carbon storage and atmospheric exchange by west Siberian peatlands*, 169 pp., Physical Geography, Universiteit Utrecht, Utrecht.

Borren, W., and W. Bleuten (2006), Simulating Holocene carbon accumulation in a western Siberian watershed mire using a three-dimensional dynamic modeling approach, *Water Resources Research*, *42*(W12413), doi:10.1029/2006WR004885.

Borren, W., W. Bleuten, and E. D. Lapshina (2004), Holocene peat and carbon accumulation rates in the southern taiga of western Siberia, *Quaternary Research*, *61*(1), 42-51.

Bubier, J. L. (1991), Patterns of Picea mariana (black spruce) growth and raised bog development in Victory Basin, Vermont, *Bulletin of the Torrey Botanical Club*, *118*(4), 399-411.

Bubier, J. L., P. Crill, A. Mosedale, S. Frolking, and E. Linder (2003), Peatland responses to varying interannual moisture conditions as measured by automatic CO_2 chambers, *Global Biogeochemical Cycles*, *17*(2, 1066), doi:10.1029/2002GB001946.

Chapman, S. J., J. Bell, D. Donnelly, and A. Lilly (2009), Carbon stocks in Scottish peatlands, *Soil Use and Management*, *25*(2), 105-112.

Charman, D. J. (2002), *Peatlands and environmental change*, 301 pp., John Wiley & Sons Ltd., Chichester.

Charman, D. J. (2007), Summer water deficit variability controls on peatland water-table changes: implications for Holocene palaeoclimate reconstructions, *The Holocene*, *17*(2), 217-227.

Clymo, R. S. (1984), The limits to peat bog growth, *Philosophical Transactions of the Royal Society of London. Series B, Biological Sciences*, *303*(1117), 605-654.

Clymo, R. S., J. Turunen, and K. Tolonen (1998), Carbon accumulation in peatland, *Oikos*, *81*(2), 368-388.

Dean, W. E. (1974), Determination of carbonate and organic matter in calcareous sediments and sedimentary rocks by loss on ignition; comparison with other methods, *Journal of Sedimentary Research*, *44*(1), 242-248.

Dorrepaal, E., S. Toet, R. S. P. van Logtestijn, E. Swart, M. J. van de Weg, T. V. Callaghan, and R. Aerts (2009), Carbon respiration from subsurface peat accelerated by climate warming in the subarctic, *Nature*, *460*(7255), 616-619.

Dyke, A. S., A. Moore, and L. Robertson (2003), Deglaciation of North America*Rep. Open File 1547*, Geological Survey of Canada, Natural Resources Canada, Ottawa.

Eppinga, M. B., M. Rietkerk, M. J. Wassen, and P. C. De Ruiter (2009), Linking habitat modification to catastrophic shifts and vegetation patterns in bogs, *Plant Ecology*, *200*, 53-68.

Frolking, S., and N. T. Roulet (2007), Holocene radiative forcing impact of northern peatland carbon accumulation and methane emissions, *Global Change Biology*, *13*(5), 1079-1088.

Glaser, P. H., B. Hansen, C. S., D. I. Siegel, A. S. Reeve, and P. J. Morin (2004), Rates, pathways and drivers for peatland development in the Hudson Bay Lowlands, northern Ontario, Canada, *Journal of Ecology*, *92*(6), 1036-1053.

Gorham, E. (1991), Northern peatlands: role in the carbon cycle and probable responses to climatic warming, *Ecological Applications*, *1*(2), 182-195.

Gorham, E., J. A. Janssens, and P. H. Glaser (2003), Rates of peat accumulation during the postglacial period in 32 sites from Alaska to Newfoundland, with special emphasis on northern Minnesota, *Canadian Journal of Botany*, *81*(5), 429-438.

Grenier, M., S. Labrecque, M. Garneau, and A. Tremblay (2008), Object-based classification of a SPOT-4 image for mapping wetlands in the context of greenhouse gases emissions: the case of the Eastmain region, Québec, Canada, *Canadian Journal of Remote Sensing*, *34*(2), S398-S314.

Haslett, J., and A. Parnell (2008), A simple monotone process with application to radiocarbon-dated depth chronologies, *Journal of the Royal Statistical Society: Series C*, *57*(4), 399-418.

Heiri, O., A. F. Lotter, and G. Lemcke (2001), Loss on ignition as a method for estimating organic and carbonate content in sediments: reproducibility and comparability of results, *Journal of Paleolimnology*, *25*(1), 101-110.

Hellberg, E., M. Niklasson, and A. Granström (2004), Influence of landscape structure on patterns of forest fires in boreal forest landscapes in Sweden, *Canadian Journal of Forest Research*, *34*, 332-338.

Hutchinson, M. F., D. W. McKenney, K. Lawrence, J. H. Pedlar, R. F. Hopkinson, E. Milewska, and P. Papadopol (2009), Development and testing of Canada-wide interpolated spatial models of daily minimum–maximum temperature and precipitation for 1961–2003, *Journal of Applied Meteorology and Climatology*, *48*, 725-741.

Jol, H. M., and C. S. Bristow (2003), GPR in sediments: advice on data collection, basic processing and interpretation, a good practice guide, *Geological Society, London, Special Publications*, *211*(1), 9-27.

Jones, M. C., and Z. Yu (2010), Rapid deglacial and early Holocene expansion of peatlands in Alaska, *Proceedings of the National Academy of Sciences*, *107*(16), 7347-7352.

Korhola, A. (1994), Radiocarbon evidence for rates of lateral expansion in raised mires in southern Finland, *Quaternary Research*, *42*(3), 299-307.

Korhola, A., M. Ruppel, H. Seppä, M. Väliranta, T. Virtanen, and J. Weckström (2010), The importance of northern peatland expansion to the late-Holocene rise of atmospheric methane, *Quaternary Science Reviews*, *29*(5-6), 611-617.

Kuhry, P., and D. H. Vitt (1996), Fossil carbon/nitrogen ratios as a measure of peat decomposition, *Ecology*, *77*(1), 271-275.

Lavoie, M., D. Paré, and Y. Bergeron (2005), Impact of global change and forest management on carbon sequestration in northern forested peatlands, *Environmental Reviews*, *13*, 199-240.

Loisel, J., and M. Garneau (2010), Late Holocene paleoecohydrology and carbon accumulation estimates from two boreal peat bogs in eastern Canada: Potential and limits of multi-proxy archives, *Palaeogeography, Palaeoclimatology, Palaeoecology*, *291*(3-4), 493-533.

MacDonald, G. M., D. W. Beilman, K. V. Kremenetski, Y. Sheng, L. C. Smith, and A. A. Velichko (2006), Rapid early development of circumarctic peatlands and atmospheric CH_4 and CO_2 variations, *Science*, *314*(5797), 285-288.

Mäkilä, M. (1997), Holocene lateral expansion, peat growth and carbon accumulation on Haukkasuo, a raised bog in southeastern Finland, *Boreas*, *26*(1), 1-14.

Mäkilä, M., and M. Moisanen (2007), Holocene lateral expansion and carbon accumulation of Luovuoma, a northern fen in finnish Lapland, *Boreas*, *36*(2), 198-210.

Mäkilä, M., and T. Goslar (2008), The carbon dynamics of surface peat layers in southern and central boreal mires of Finland and Russian Karelia, *Suo*, *59*(3), 49-69.

Malmer, N., and B. Wallén (1999), The dynamics of peat accumulation on bogs: mass balance of hummocks and hollows and its variation throughout a millennium, *Ecography*, *22*(6), 736-750.

Mauquoy, D., T. Engelkes, M. H. M. Groot, F. Markesteijn, M. G. Oudejans, J. van der Plicht, and B. van Geel (2002), High-resolution records of late-Holocene climate change and carbon accumulation in two north-west European ombrotrophic peat bogs, *Palaeogeography, Palaeoclimatology, Palaeoecology*, *186*(3-4), 275-310.

Neal, A. (2004), Ground-penetrating radar and its use in sedimentology: principles, problems and progress, *Earth-Science Reviews*, *66*(3-4), 261-330.

Nilsson, M., M. Klarqvist, E. Bohlin, and G. Possnert (2001), Variation in ^{14}C age of macrofossils and different fractions of minute peat samples dated by AMS, *The Holocene*, *11*(5), 579-586.

Nordbakken, J.-F. (1996), Plant niches along the water-table gradient on an ombrotrophic mire expanse, *Ecography*, *19*(2), 114-121.

Payette, S. (1988), Late-Holocene development of subarctic ombrotrophic peatlands: allogenic and autogenic succession, *Ecology*, *69*(2), 516-531.

Payette, S., and L. Rochefort (2001), *Écologie des tourbières du Québec-Labrador*, 621 pp., Les presses de l'Université Laval, Ste-Foy.

Pelletier, L., M. Garneau, and T. R. Moore (in review), Interannual variation in net ecosystem exchange at the microform scale in a boreal bog, Eastmain region, Quebec, Canada, *Journal of Geophysical Research - Biogeosciences*.

Peters, M. E., and P. E. Higuera (2007), Quantifying the source area of macroscopic charcoal with a particle dispersal model, *Quaternary Research*, *67*(2), 304-310.

Pitkänen, A., J. Turunen, and K. Tolonen (1999), The role of fire in the carbon dynamics of a mire, eastern Finland, *The Holocene*, *9*(4), 453-462.

Plummer, D. A., D. Caya, A. Frigon, H. Côté, M. Giguère, D. Paquin, S. Biner, R. Harvey, and R. de Elia (2006), Climate and climate change over North America as simulated by the Canadian RCM, *Journal of Climate*, *19*(13), 3112-3132.

Reimer, P. J., et al. (2004), INTCAL04 terrestrial radiocarbon age calibration, 0–26 cal kyr BP, *Radiocarbon*, *46*(3), 1029-1058.

Rosa, E., M. Larocque, S. Pellerin, S. Gagné, and B. Fournier (2009), Determining the number of manual measurements required to improve peat thickness estimations by ground penetrating radar, *Earth Surface Processes and Landforms*, *34*(3), 377-383.

Roulet, N. T. (2000), Peatlands, carbon storage, greenhouse gases, and the Kyoto protocol: prospects and significance for Canada, *Wetlands*, *20*(4), 605-615.

Rydin, H. (1993), Interspecific competition between Sphagnum mosses on a raised bog, *Oikos*, *66*(3), 413-423.

Sandmeier, K. J. (2005), Reflexw 3.5.7. Manual, edited, Sandmeier Software, Karlsruhe.

Saucier, J.-P., J.-F. Bergeron, P. Grondin, and A. Robitaille (1998), Les régions écologiques du Québec méridional (3e version): un des éléments du système hiérarchique de classification écologique du territoire mis au point par le ministère des Ressources naturelles du Québec, *L'Aubelle*, *124*, 1-12.

Schimel, D. S., et al. (2001), Recent patterns and mechanisms of carbon exchange by terrestrial ecosystems, *Nature*, *414*, 169-172.

Sheng, Y., L. C. Smith, G. M. MacDonald, K. V. Kremenetski, K. E. Frey, A. A. Velichko, M. Lee, D. W. Beilman, and P. Dubinin (2004), A high-resolution GIS-based inventory of the west Siberian peat carbon pool, *Global Biogeochemical Cycles*, *18*.

Swanson, D. K. (2007), Interaction of mire microtopography, water supply, and peat accumulation in boreal mires, *Suo*, *58*(2), 37-47.

Tolonen, K., and J. Turunen (1996), Accumulation rates of carbon in mires in Finland and implications for climate change, *The Holocene*, *6*(2), 171-178.

Troels-Smith, J. (1955), Characterization of unconsolidated sediments *Danmarks Geologiske Undersogelse, Series IV*, *3*, 38-73.

Turetsky, M., K. Wieder, L. Halsey, and D. Vitt (2002), Current disturbance and the diminishing peatland carbon sink, *Geophysical Research Letters*, *29*(11, 1526), doi:10.1029/2001GL014000.

Turetsky, M. R., and R. K. Wieder (2001), A direct approach to quantifying organic matter lost as a result of peatland wildfire, *Canadian Journal of Forest Research*, *31*, 363-366.

Turunen, J., T. Tahvanainen, K. Tolonen, and A. Pitkänen (2001), Carbon accumulation in West Siberian mires, Russia, *Global Biogeochemical Cycles*, *15*(2), 285-296.

Turunen, J., E. Tomppo, K. Tolonen, and A. Reinikainen (2002), Estimating carbon accumulation rates of undrained mires in Finland-application to boreal and subarctic regions, *The Holocene*, *12*(1), 69-80.

Turunen, J., N. T. Roulet, T. R. Moore, and P. J. H. Richard (2004), Nitrogen deposition and increased carbon accumulation in ombrotrophic peatlands in eastern Canada, *Global Biogeochemical Cycles*, *18*(GB3002), doi:10.1029/2003GB002154.

Vardy, S. R., B. G. Warner, J. Turunen, and R. Aravena (2000), Carbon accumulation in permafrost peatlands in the Northwest Territories and Nunavut, Canada, *The Holocene*, *10*(2), 273-280.

Viau, A. E., K. Gajewski, M. C. Sawada, and P. Fines (2006), Millennial-scale temperature variations in North America during the Holocene, *Journal of Geophysical Research*, *111*.

Vitt, D. H., L. A. Halsey, I. E. Bauer, and C. Campbell (2000), Spatial and temporal trends in carbon storage of peatlands of continental western Canada through the Holocene, *Canadian Journal of Earth Sciences*, *37*(5), 683-693.

Waddington, J. M., and N. T. Roulet (1999), Carbon balance of a boreal patterned peatland, *Global Change Biology*, *6*, 87-97.

Yu, Z. (2006), Holocene carbon accumulation of fen peatlands in boreal western Canada: a complex ecosystem response to climate variation and disturbance, *Ecosystems*, *9*(8), 1278-1288.

Yu, Z., D. W. Beilman, and M. C. Jones (2009), Sensitivity of northern peatland carbon dynamics to Holocene climate change, in *Carbon cycling in northern peatlands*, edited by A. J. Baird, L. R. Belyea, X. Comas, A. S. Reeve and L. D. Slater, pp. 55-69, American Geophysical Union, Washington.

Yu, Z., D. H. Vitt, I. D. Campbell, and M. J. Apps (2003), Understanding Holocene peat accumulation pattern of continental fens in western Canada, *Canadian Journal of Botany*, *81*, 267-282.

Yu, Z., J. Loisel, D. P. Brosseau, D. W. Beilman, and S. J. Hunt (2010), Global peatland dynamics since the Last Glacial Maximum, *Geophysical Research Letters*, *37*(13), L13402.

Zoltai, S. C. (1995), Permafrost distribution in peatlands of West-Central Canada during the Holocene Warm Period 6000 years BP, *Géographie physique et Quaternaire*, *49*(1), 45-54.

Figure captions

Figure 1: Location of the Eastmain region within eastern Canada and studied peatlands.

Figure 2: Peat cover thickness models and profiles for each peatland.

Figure 3: Age-depth models for each of the peatlands. Grey lines indicate the limits of the 95% confidence interval.

Figure 4: Mean C density since 2000 cal BP for each peatland. Brackets indicate the standard error.

Figure 5: Peatland vegetation types for each peatland. Columns show *Sphagnum* peat (dark grey), moss (non-*Sphagnum*) peat (light grey), herbaceous peat (white), wood peat (v-symbol) and unidentifiable organic matter (black).

Figure 6: Peatland lateral expansion rates during the Holocene. Black line represents smoothing.

Figure 7: Holocene C flux for each of the peatlands.

Tables

Table 1: Radiocarbon datings for dated samples, listed per peatland and core.

Sph = *Sphagnum* spp.; Eric = Ericaceae; Cyp = Cyperaceae.

Site	Core	Sample depth (cm)	Laboratory number	Material	^{14}C age (BP)	2σ range (cal BP)	Age (cal BP)
LLC	C	51-52	UCIAMS43480	Sph stems	340±20	317-480	391
	C	77-78	UCIAMS58634	Sph stems	915±15	777-906	846
	C	102-103	UCIAMS50203	Sph stems	1205±15	1072-1225	1140
	C	120-121	UCIAMS57419	Sph stems	1980±15	1872-1991	1924
	C	140-141	UCIAMS57421	Sph stems	2550±15	2531-2748	2716
	C	153-154	UCIAMS50204	Sph stems	2915±15	2984-3155	3057
	C	201-202	UCIAMS43479	Sph stems	3745±20	3996-4171	4107
	C	250-251	UCIAMS58636	Sph stems	4165±20	4596-4819	4701
	C	293-294	UCIAMS50205	Sph stems	4450±15	4980-5265	5110
	C	351-352	UCIAMS43478	Sph stems	4985±20	5653-5844	5701
	C	439-440	UCIAMS50206	Sph stems	6055±15	6821-6968	6912
	C	480-483	Beta223743	Eric leaf frs	6640±40	7431-7627	7520
	L1	45-46	UCIAMS58637	Sph stems	630±15	551-670	601
	L1	58-59	UCIAMS54956	Sph stems	1250±30	1078-1289	1207
	L1	68-69	UCIAMS58639	Sph stems, Larix/Picea leaf frs	1940±20	1810-1975	1889
	L1	99-100	UCIAMS57423	Sph stems	3125±15	3255-3390	3355
	L1	112-113	UCIAMS58638	Sph stems	3395±15	3586-3702	3656
	L1	130-131	UCIAMS54955	Sph stems	3780±25	4056-4269	4162
	L1	170-171	UCIAMS57418	Sph stems	4625±15	5295-5447	5418

	L1	210-211	UCIAMS64581	Sph stems	5035±20	5721-5903	5841
	L1	249-254	UCIAMS40365	Sph stems, Eric leaf frs	6055±20	6673-7218	6908
	L2	100-101	UCIAMS40366	Picea leaf frs	3690±20	3971-4098	4035
	L3	258-261	UCIAMS40367	Picea/Eric leaf frs	5500±20	6275-6383	6329
	L4	39-40	UCIAMS57417	Sph stems, Eric/Picea leaf frs	190±15	151-294	198
	L4	52-53	UCIAMS58632	Sph stems	1070±15	933-1075	978
	L4	61-63	UCIAMS58633	Sph stems, Eric leaf frs	1405±20	1216-1427	1301
	L4	78-79	UCIAMS57415	Sph stems, Larix/Eric leaf frs	2170±15	2129-2317	2152
	L4	127-128	UCIAMS57422	Sph stems	3135±15	3342-3435	3351
	L4	147-148	UCIAMS58635	Sph stems, Eric/Larix leaf frs	3495±20	3670-3826	3769
	L4	188-189	UCIAMS40368	Sph stems	4120±20	4520-4788	4586
	T1	47-48	UCIAMS64582	Sph stems	105±20	34-262	126
	T1	53-54	UCIAMS54957	Sph stems	300±25	304-691	410
	T1	77-80	UCIAMS54954	Sph stems	3440±25	3007-4270	3684
	T4	45-46	UCIAMS57416	Sph stems	180±15	14-283	189
	T4	55-56	UCIAMS64583	Sph stems/Picea leaf frs	325±20	319-488	410
	T4	70-71	UCIAMS57420	Sph stems	1250±15	1095-1293	1211
MOS	C	40-41	UCIAMS57424	Sph stems	355±15	325-522	444
	C	70-71	UCIAMS54958	Sph stems	1270±25	1095-1313	1223
	C	95-96	UCIAMS64586	Sph stems	1990±20	1837-1985	1924
	C	108-109	UCIAMS67515	Sph stems	2065±25	1976-2119	2043
	C	120-121	UCIAMS54959	Sph stems	2225±25	2157-2335	2237
	C	136-137	UCIAMS64588	Sph stems	2490±20	2478-2728	2591
	C	172-173	UCIAMS54960	Sph stems	3275±25	3405-3604	3506
	C	224-225	UCIAMS54961	Sph stems	4185±25	4609-4863	4739
	C	246-247	UCIAMS57426	Sph stems	4740±15	5333-5634	5534
	C	296-297	Beta223744	Sph stems	6200±40	6936-7237	7072
	L1	55-56	UCIAMS65378	Charcoal frs	190±15	149-310	229
	L1	77-78	UCIAMS65385	Charcoal frs	1260±20	1100-1282	1216
	L1	89-90	UCIAMS65389	Charcoal frs	1840±20	1705-1907	1781
	L1	117-119	UCIAMS65386	Charcoal, Cyp seeds	3625±20	3067-3983	3897
	L1	141-144	UCIAMS65375	Charcoal, Cyp seeds; Picea leaf frs	3070±20	3418-4734	Rejected
	L1	167-170	UCIAMS43474	Eric leaf frs; Cyp seeds	6420±20	6799-7749	7340
	L2	160-164	UCIAMS43475	Picea leaf frs	5655±20	6401-6484	6443
	L3	211-213	UCIAMS40364	Sph stems	5755±20	6491-6630	6561
	L4	51-52	UCIAMS57425	Sph stems	455±15	502-550	545
	L4	73-74	UCIAMS58642	Sph stems	2165±20	2097-2285	2130
	L4	97-99	UCIAMS58641	Eric/Larix leaf frs	2750±20	2790-2911	2852
	L4	136-137	UCIAMS58640	Eric/Larix/Picea leaf frs	3835±15	4162-4326	4322
	L4	169-170	UCIAMS43476	Sph stems	4670±20	5318-5457	5323
	T4	24-25	UCIAMS64584	Charcoal	165±20	170-476	210
	T4	67-68	UCIAMS64589	Charcoal	2670±20	2342-2834	2794
	T4	83-84	UCIAMS65379	Charcoal	4055±20	3997-4603	4407
STE	C	45-46	UCIAMS54962	Sph stems	105±30	75-260	116
	C	67-68	UCIAMS58645	Picea leaf frs	600±20	548-646	620
	C	79-80	UCIAMS64589	Sph stems	1175±20	1039-1166	1112
	C	98-99	UCIAMS54963	Sph stems	1715±25	1568-1697	1578
	C	124-125	UCIAMS65381	Sph stems	2445±20	2351-2663	2461
	C	160-161	UCIAMS54964	Sph stems	3255±30	3316-3521	3505
	C	179-180	UCIAMS67514	Sph stems	3415±25	3588-3671	3597
	C	194-195	UCIAMS58644	Sph stems	3125±15	3654-3763	Rejected
	C	201-202	UCIAMS65382	Sph stems	3485±20	3757-3912	3805
	C	223-224	UCIAMS54965	Sph stems	3960±30	4283-4431	4362
	C	239-240	UCIAMS58643	Sph stems/Picea leaf frs	3975±15	4422-4685	4424

C	285-286	UCIAMS40360	Sph stems	6225±20	6731-7219	7007
L1	161-165	UCIAMS40361	Sph stems; Cyp seeds; Picea leaf frs	6215±20	7016-7238	7127
L2	44-45	UCIAMS67506	Sph stems	265±25	269-436	316
L2	68-69	UCIAMS67507	Sph stems	1195±25	1031-1232	1123
L2	98-99	UCIAMS67508	Sph stems	2380±25	2329-2588	2399
L2	142-143	UCIAMS67509	Sph stems	3200±25	3360-3471	3415
L2	180-181	UCIAMS67510	Sph stems	3820±25	4108-4363	4207
L2	212-213	UCIAMS67511	Sph stems	4465±25	4977-5288	5182
L2	244-246	UCIAMS40362	Sph stems	5760±20	6412-6725	6550
L3	135-139	UCIAMS43477	Picea/Eric leaf frs	5215±20	5924-5995	5960
L4	35-36	UCIAMS65384	Sph stems	135±20	70-287	224
L4	48-49	UCIAMS67512	Charcoal frs	945±25	778-967	867
L4	63-64	UCIAMS65380	Charcoal; Picea leaf frs	2455±20	2343-2708	2524
L4	84-85	UCIAMS67513	Charcoal frs	3540±25	3703-3948	3826
L4	125-126	UCIAMS65376	Charcoal, Picea/Eric leaf frs	5490±20	6189-6339	6288
L4	174-176	UCIAMS40363	Sph stems; Larix leaf frs; Cyp seeds	6185±20	6976-7345	7090
T4	46-47	UCIAMS65383	Sph stems	165±20	135-328	225
T4	63-64	UCIAMS65377	Charcoal frs	1660±20	1442-1789	1557

Table 2: Peatland characteristics. Standard errors are in parentheses.

	LLC	MOS	STE
Surface area (km^2)	2.241	2.672	1.722
Mean peat thickness (m)	2.50	1.82	1.87
Peat volume (10^6 m^3)	5.614	4.864	3.225
Mean C density (kg m^{-3})	42.5 (0.363)	44.5 (0.427)	45.8 (0.559)
Present – 250 cal BP	32.2 (0.600)	33.5 (0.705)	32.8 (0.993)
250 cal BP – mineral base	46.0 (0.387)	48.9 (0.438)	51.6 (0.556)
Mean C mass per area (kg m^{-2})	106.4	81.0	85.8
Total C mass (10^6 kg)	242.4	216.8	148.5
Mean basal age (cal BP)	5664	5576	5636
Holocene C accumulation rate (g m^{-2} yr^{-1})	18.9	14.4	15.2
Recent C accumulation rate (g m^{-2} yr^{-1})	53.9	55.8	59.4

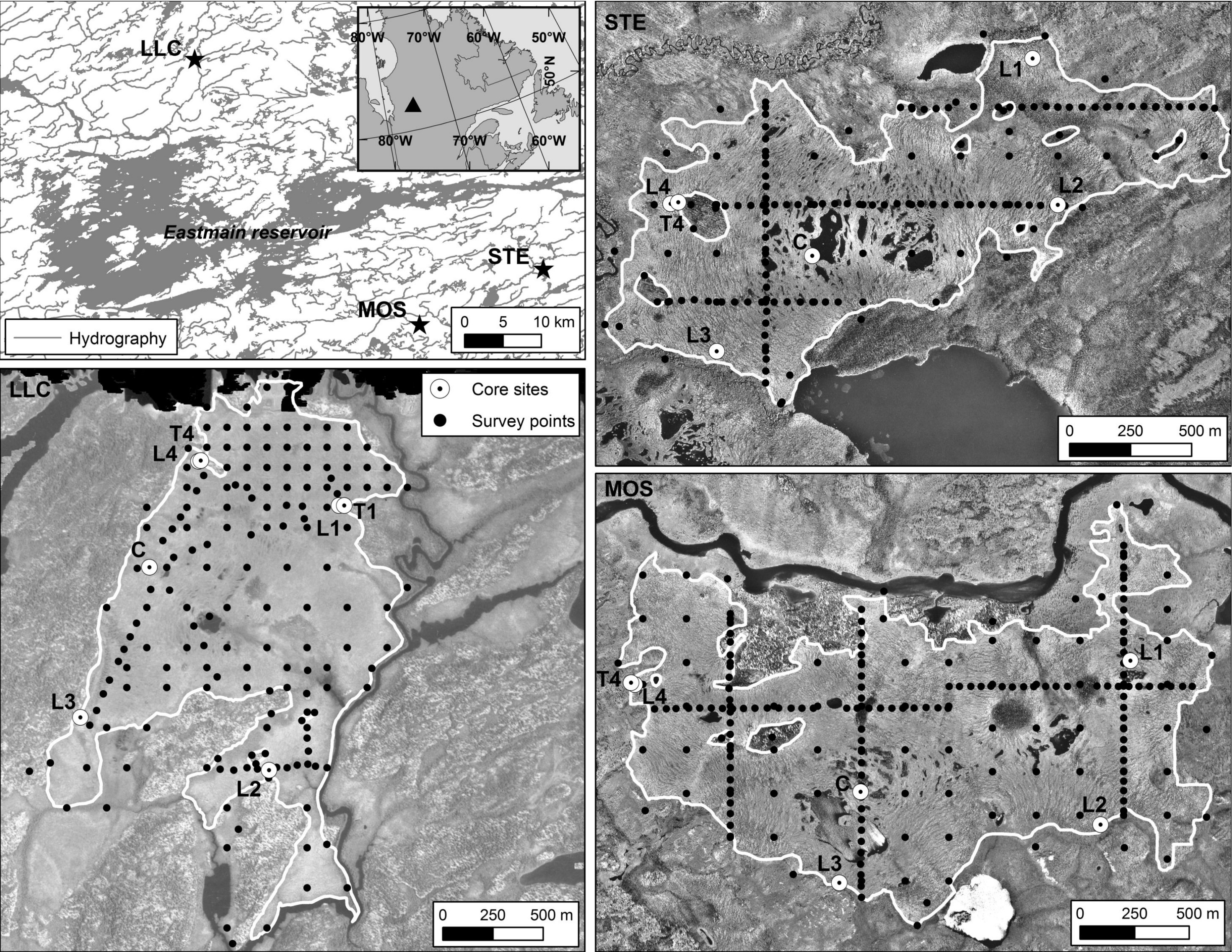
LLC
STE
MOS
80°W
70°W
60°W
50°W
50°N
Eastmain reservoir
Hydrography
0
5
10 km
L1
L2
L3
L4
T4
T1
C
Core sites
Survey points
0
250
500 m

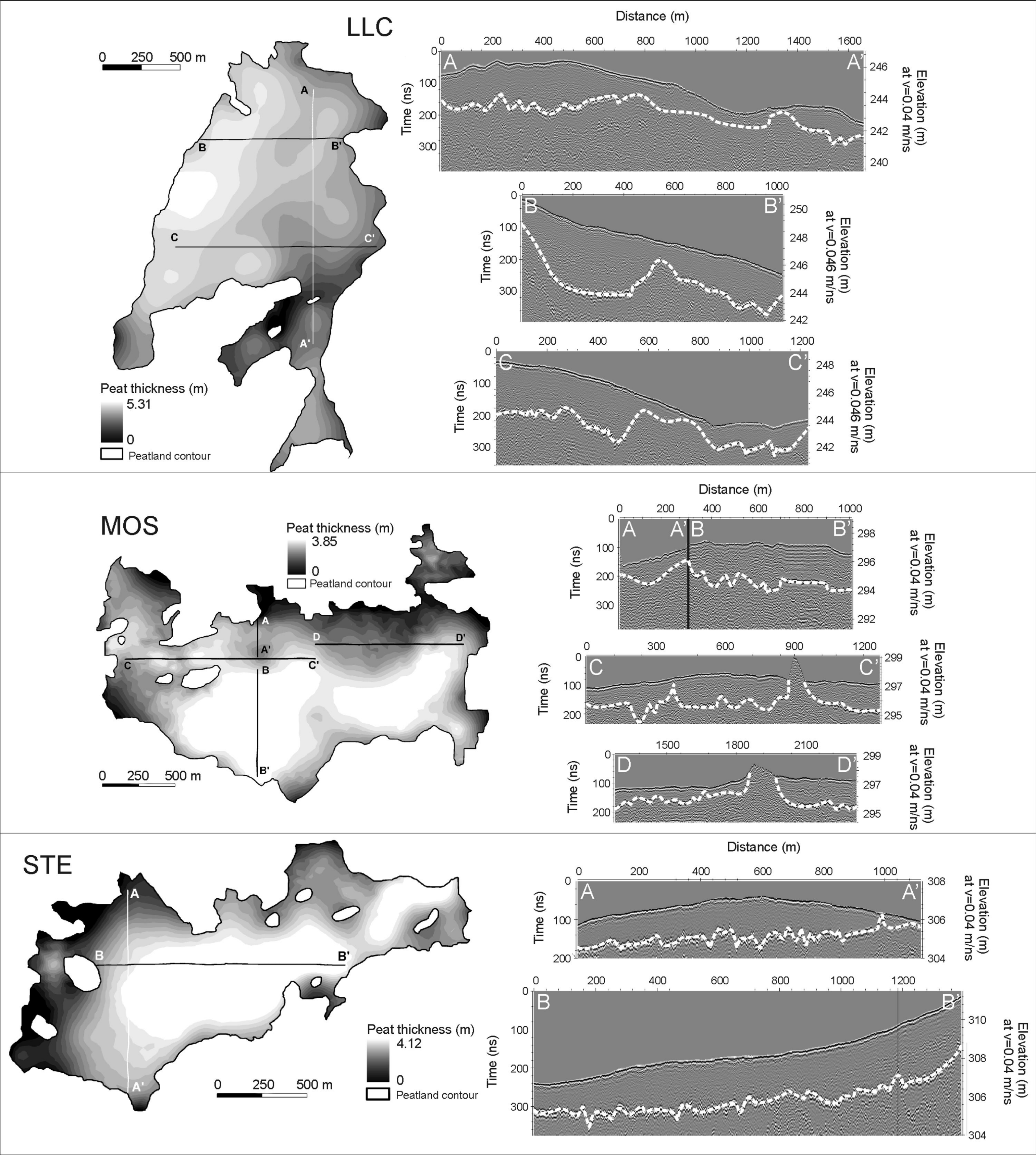

LLC
0 250 500 m
Peat thickness (m)
5.31
0
Peatland contour
Distance (m)
Time (ns)
Elevation (m) at v=0.04 m/ns
Elevation (m) at v=0.046 m/ns
MOS
Peat thickness (m)
3.85
0
Peatland contour
0 250 500 m
Distance (m)
Time (ns)
Elevation (m) at v=0.04 m/ns
STE
Peat thickness (m)
4.12
0
Peatland contour
0 250 500 m
Distance (m)
Time (ns)
Elevation (m) at v=0.04 m/ns

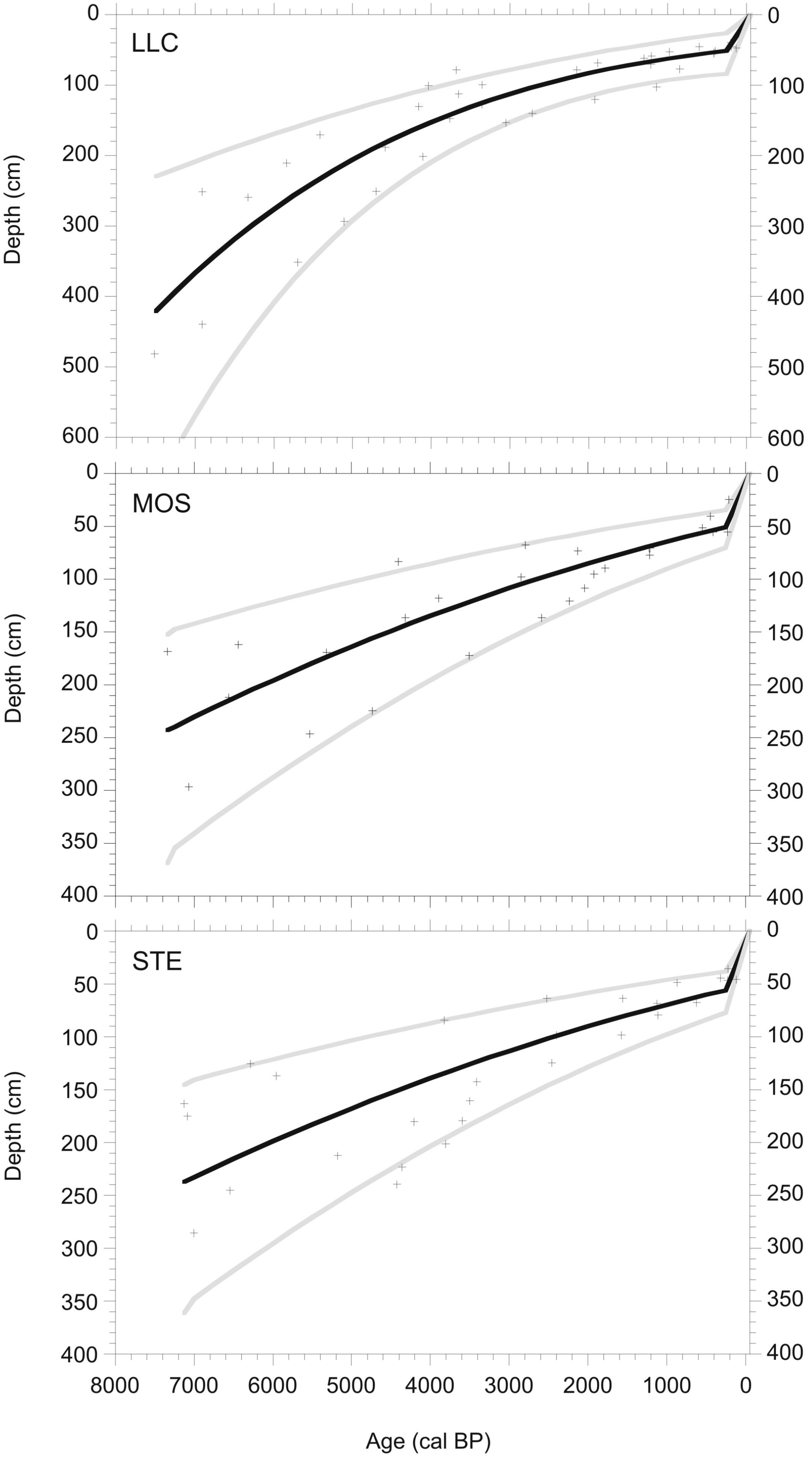

LLC
MOS
STE
Depth (cm)
Age (cal BP)
0
100
200
300
400
500
600
50
150
250
350
8000
7000
6000
5000
4000
3000
2000
1000

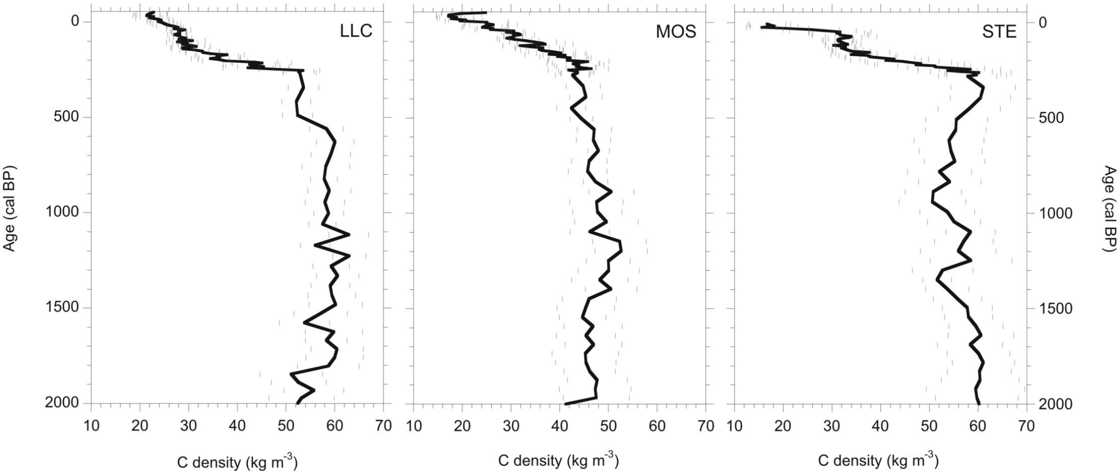
LLC
MOS
STE
Age (cal BP)
C density (kg m^{-3})
0
500
1000
1500
2000
10
20
30
40
50
60
70

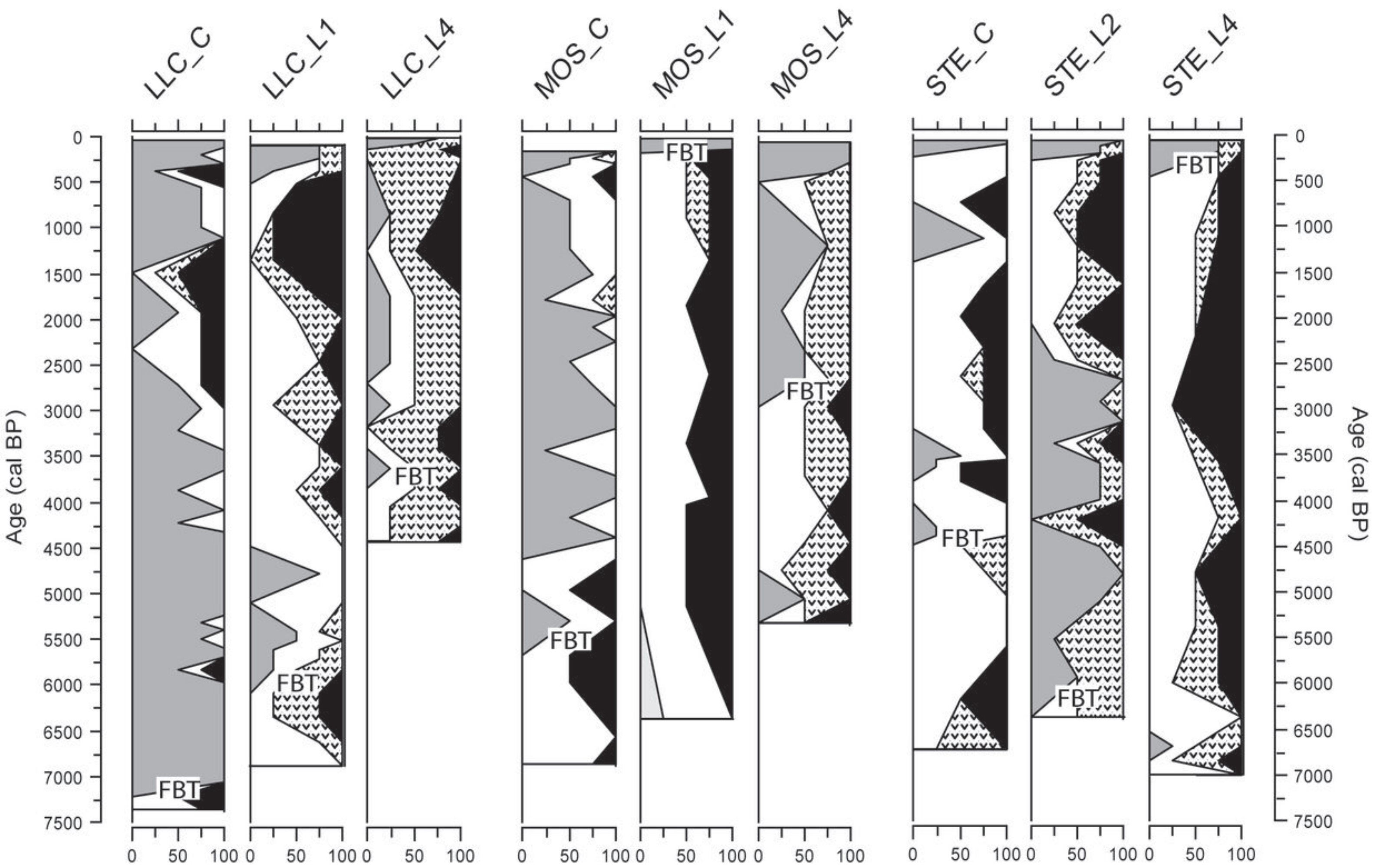

LLC_C
LLC_L1
LLC_L4
MOS_C
MOS_L1
MOS_L4
STE_C
STE_L2
STE_L4
Age (cal BP)
0
500
1000
1500
2000
2500
3000
3500
4000
4500
5000
5500
6000
6500
7000
7500
FBT
0 50 100

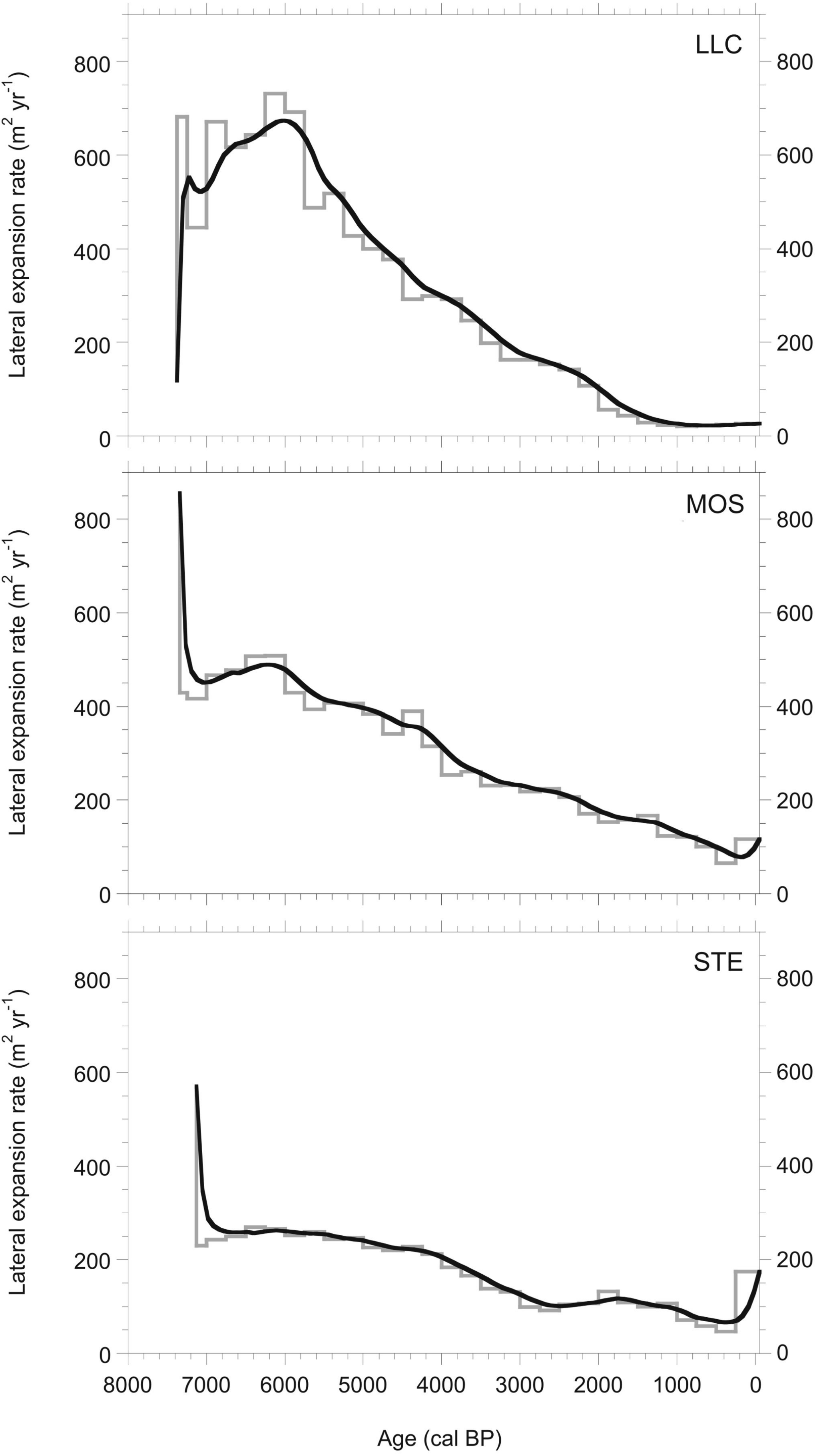
LLC
MOS
STE
Lateral expansion rate (m^2 yr^{-1})
0
200
400
600
800
8000
7000
6000
5000
4000
3000
2000
1000
0
Age (cal BP)

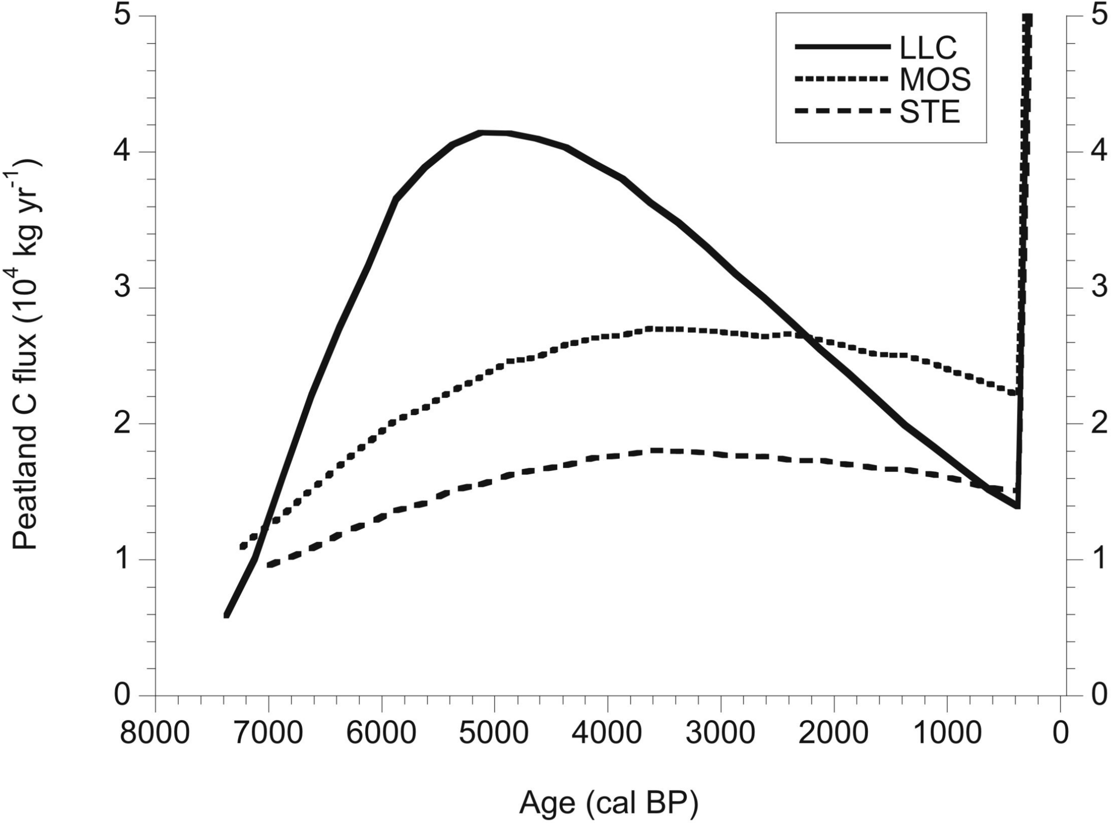
LLC
MOS
STE
Peatland C flux (10^4 kg yr^{-1})
Age (cal BP)
0
1
2
3
4
5
8000
7000
6000
5000
4000
3000
2000
1000
0